ORGANOMETALLICS

ARTICLE

pubs.acs.org/Organometallics

Impact of Cyclometalation and π-Conjugation on Photoisomerization of an N,C-Chelate Organoboron Compound

Ying-Li Rao and Suning Wang*

Department of Chemistry, Queen's University, Kingston, Ontario, K7L 3N6, Canada

Supporting Information

ABSTRACT: N,C-Chelate four-coordinate boron compounds that contain a B(ppy)Mes_2 unit (ppy = 2-phenylpyridyl, Mes = mesityl) are a new class of photochromic molecules discovered recently by our group that undergo photoisomerization upon exposure to light. To examine the influence of a covalently bound transition metal ion on the photochromic properties of this class of boron compounds, a new molecule (**L1**) that contains two linearly conjugated ppy units has been synthesized. A $BMes_2$ group was attached to **L1** via chelation with one of the ppy units, producing a new four-coordinate boron compound, **B1**. The reactions of **B1** with $PtPh_2(DMSO)_2$ produced a Pt(II) cyclometalated compound, **Pt1**, where a PtPh(DMSO) unit is bound to the second ppy unit of **B1**. Replacement of DMSO in **Pt1** by *p*-*t*-Bu-pyridine provided a new compound, **Pt2**. A third Pt(II) compound, **Pt3**, where a Pt(dpm) group (dpm = dipivaloylmethane) is chelated to the second ppy site of **B1**, was also synthesized successfully. The crystal structures of **B1** and **Pt3** have been determined by single-crystal X-ray diffraction analyses. The photophysical and photochromic properties of **B1** and **Pt1**−**Pt3** have been examined. Experimental and computational studies established that Pt(II) cyclometalation to **B1** stabilizes a ^{3}LC state that involves $\pi\rightarrow\pi^*$ transitions localized on the ppy−ppy conjugated backbone. This ^{3}LC state of the Pt(II) compounds is highly phosphorescent, with quantum efficiencies being 0.16, 0.13, and 0.45 for **Pt1**, **Pt2**, and **Pt3**, respectively, in toluene and at ambient temperature. The B(ppy)Mes_2 chromophore in all three Pt(II) compounds has been found to undergo photoisomerization in a similar manner to that of **B1**, but with a much lower quantum efficiency than **B1**. Deactivation of the photoisomerization process by the ^{3}LC state has been found to be most likely responsible for the low photoisomerization quantum efficiency of the Pt(II) compounds.

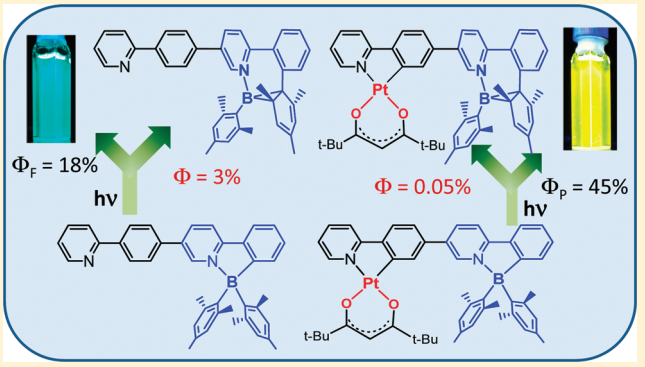

INTRODUCTION

Organoboron compounds have important applications in optoelectronic devices[1−3] including organic light emitting diodes (OLEDs),[2] probes, and sensors.[3] Our recent discovery on an unusual photochromic switching phenomenon of four-coordinate N,C-chelate organoboron compounds[4] with the general formula B(N,C-chelate)Mes_2 (Mes = mesityl) added a new dimension to organoboron-based materials chemistry. The influence of transition metal coordination on photochromic properties of well-established systems such as azobenzene[5] and diarylethene (DTE)[6] has been studied extensively. It has been shown that by choosing appropriate metal ions and the linker, it is possible to sensitize the photochromic switching through the excited state of the metal chromophore for systems such as DTE.[5,6] To examine if the attachment of a metal center has any impact on the photochromic properties of a N,C-chelate boron compound such as[4a] B(ppy)Mes_2 (ppy = 2-phenylpyridyl), we have synthesized a new conjugated photochromic organoboron compound and several of its cyclometalated N,C-chelate Pt(II) compounds. The N,C-chelate Pt(II) chromophore is chosen because the energy of its emissive state is usually dominated by the ^{3}LC (ligand-centered) transition of the chelate ligand,[7] which may be directly coupled to the B(ppy)Mes_2 chromophore, thus modulating the photochromic properties of the boron compound. Furthermore, the ancillary ligands on the Pt(II) center allow the tuning of the energy of the metal-to-ligand charge transfer (MLCT) transition and its influence on the properties of the boron center. The ligand we designed for this study is a π-conjugated molecule, **B1** (Chart 1), where the N,C-chelate site for the Pt(II) center is directly conjugated with the photochromic boron group. The details of our investigation on **B1** and its Pt(II) complexes are presented herein.

EXPERIMENTAL SECTION

General Procedures. All reactions were performed under N_2 with standard Schlenk techniques unless otherwise noted. All starting materials were purchased from Aldrich Chemical Co. and used without further purification. DMF, THF, Et_2O, and hexanes were purified using an Innovation Technology Co. solvent purification system. CH_2Cl_2 was freshly distilled over phosphorus pentoxide prior to use. Deuterated

Received: June 21, 2011
Published: July 20, 2011

solvents were purchased from Cambridge Isotopes and were used as received without further drying. NMR spectra were recorded on Bruker Avance 400 or 500 MHz spectrometers. $[PtPh_2(DMSO)_2]$ was synthesized according to a literature method.[8] UV−vis spectra were recorded on an Ocean Optics UV−visible spectrometer. Excitation and emission spectra were recorded on a Photon Technologies International QuantaMaster model C-60 spectrometer. Emission lifetimes were measured on a Photon Technologies International Phosphorescent spectrometer (Time-Master C-631F) equipped with a xenon flash lamp and digital emission photon multiplier tube using a band pathway of 5 nm for excitation and 2 nm for emission. Fluorescent quantum yields of **B1** were determined in CH_2Cl_2 using 9,10-diphenylanthracene as the standard at 298 K ($\Phi_r = 0.90$). The absorbance of all the samples and the standard at the excitation wavelength is approximately 0.096−0.109. For the Pt(II) complexes **Pt1**−**Pt3**, the phosphorescent quantum efficiency was measured under N_2 using $Ir(ppy)_3$ as the standard ($\Phi = 0.95$) in 2-Me-THF.[9]

Syntheses. As shown in Scheme 1, **B1** was synthesized by a Suzuki cross-coupling reaction between 2-(2-bromophenyl)-5-iodopyridine and 4-(pyridin-2-yl)phenylboronic acid to produce **L1**, followed by the lithiation and substitution by $BMes_2F$. The synthetic procedures for the precursor compounds 2-(2-bromophenyl)-5-iodopyridine, 2-(4-bromophenyl)pyridine, and 4-(pyridin-2-yl)phenylboronic acid of **L1** can be found in the Supporting Information.

*Synthesis of 2-(2-Bromophenyl)-5-(4-(pyridin-2-yl)phenyl)pyridine (**L1**).* This compound was synthesized using a Suzuki coupling procedure. A 10 mL amount of dry toluene was added to a solid mixture of 4-(pyridin-2-yl)phenylboronic acid (0.8 g, 4.0 mmol), 2-(2-bromophenyl)-5-iodopyridine (1.1 g, 3.0 mmol), $Pd(OAc)_2$ (13.0 mg, 0.06 mmol), 2-dicylohexylphosphino-2′,6′-dimethoxybiphenyl (50.0 mg, 0.012 mmol), and K_3PO_4 (1.2 g, 6 mmol) under nitrogen. The mixture was stirred at 60 °C for 48 h. Then 20 mL of H_2O was added to the reaction mixture, and the water layer was separated and extracted with CH_2Cl_2 (3 × 10 mL). The combined organic layers were dried over Na_2SO_4, and the solvents were evaporated under reduced pressure. Purification of the crude product by column chromatography (hexane/THF, 4:1) afforded the product as a white solid in 20% yield (0.23 g). ^{1}H NMR (400 MHz, $CDCl_3$, 25 °C, δ, ppm): 9.02 (d, J = 1.2 Hz; 1H), 8.73 (d, J = 4.8 Hz; 1H), 8.14 (d, J = 8.0 Hz; 2H), 8.01 (dd, J = 8.0 Hz, J = 2.0 Hz; 1H), 7.77 (m, 4H), 7.71 (m; 2H), 7.61 (d, J = 6.4 Hz; 1H), 7.43 (t, J = 8.0 Hz; 1H), 7.25 (m, 2H).

*Synthesis of 2-(2-(Dimesitylboryl)phenyl)-5-(4-(pyridin-2-yl)phenyl)-pyridine (**B1**).* To a stirred solution (diethyl ether/THF, 40/80 mL) of 2-(2-bromophenyl)-5-(4-(pyridin-2-yl)phenyl)pyridine (0.23 g, 0.6 mmol) at −78 °C was added dropwise via a syringe an *n*-BuLi solution (1.60 M; 0.6 mL, 1.0 mmol) over 1 min. The resulting solution was stirred for 1 h at −78 °C. Then a solution of dimesitylboron fluoride (0.36 g, 1.2 mmol) in Et_2O was quickly added. The reaction mixture was kept at −78 °C for another 1 h and then allowed to reach ambient temperature and stirred overnight. After the removal of the solvent, purification of the crude product by column chromatography (CH_2Cl_2/hexane, 1:1) afforded the product as a yellow solid in 25% yield (0.08 g). The resulting yellow solid was recrystallized avoiding light from CH_2Cl_2/hexane to give yellow crystals of **B1**. ^{1}H NMR (400 MHz, CD_2Cl_2, 25 °C, δ, ppm): 8.93 (d, J = 1.2 Hz; 1H), 8.71 (d, J = 4.8 Hz; 1H), 8.32 (dd, J = 8.0 Hz, J = 2.0 Hz; 1H), 8.17 (d, J = 8.0 Hz; 2H), 8.10 (d, J = 8.0 Hz; 1H), 7.95 (d, J = 6.4 Hz; 1H), 7.80 (t; 2H), 7.78 (d, J = 6.4 Hz; 1H), 7.63 (d, J = 8.0 Hz; 2H), 7.32 (m; 3H), 6.68 (s; 4H), 2.18 (s; 6H), 1.87 (s; 12H). ^{13}C{^{1}H}NMR (100 MHz, C_6D_6, δ, ppm): 158.16, 156.46, 150.24, 144.55, 140.10, 138.45, 136.50, 136.33, 135.07, 134.38, 134.21, 132.16, 131.62, 130.82, 129.14, 127.08, 125.64, 122.49, 121.75, 120.12, 119.56, 117.50, 114.45, 113.18, 25.70, 20.99. Anal. Calcd for $C_{40}H_{37}BN_2$: C 86.32, H 6.70, N 5.03. Found: C 86.28, H 6.87, N 5.01.

*Synthesis of **Pt1**.* To a stirred THF (20 mL) solution of $[PtPh_2(DMSO)_2]$ (51.0 mg, 0.10 mmol) was added **B1** (50 mg, 0.09 mmol). The mixture was stirred at 50 °C for 6 h, and the solvent was removed under reduced pressure. Pure **Pt1** was obtained after the residue solid was washed with hexane and ether, with 90% yield. ^{1}H NMR (400 MHz, CD_2Cl_2, 25 °C, δ, ppm): 9.70 (d, J = 4.8 Hz; 1H), 8.55 (s; 1H), 7.96 (m; 2H), 7.84 (m; 3H), 7.71 (d, J = 8.0 Hz; 2H), 7.47 (d, satellites, J_{Pt-H} = 60.0 Hz, J = 8.0 Hz; 2H), 7.73 (m; 3H), 7.18 (dd, J = 8.0 Hz, J = 1.6 Hz; 1H), 6.98 (t, J = 7.2 Hz; 2H), 6.87 (d; J = 6.8 Hz; 1H), 6.81 (d, J = 2.0 Hz; 1H), 6.64 (s; 4H), 2.94 (s, satellites; 6H), 2.18 (s; 6H), 1.76 (s; 12H). ^{13}C NMR was not recorded due to the poor solubility of **Pt1**. Anal. Calcd for $C_{49}H_{51}BN_2OPtS$: C 63.84, H 5.58, N 3.04, S 3.48. Found: C 63.68, H 5.34, N 3.11, S 3.14.

Chart 1

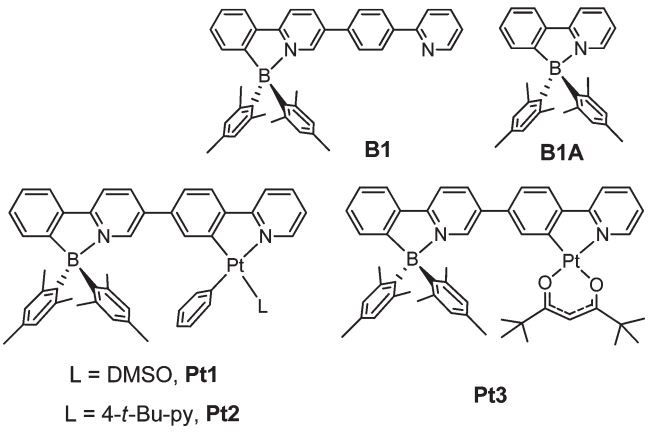

Scheme 1[a]

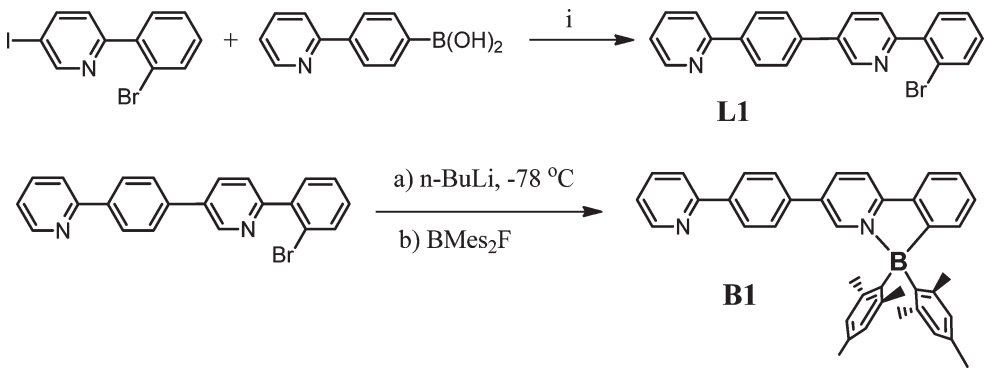

[a] Conditions: (i) $Pd(OAc)_2$, K_3PO_4, 2-dicyclohexylphosphino-2′,6′-dimethoxybiphenyl in toluene, 60 °C.

Synthesis of ***Pt2***. To a CH_2Cl_2 (20 mL) solution of **Pt1** (45 mg, 0.05 mmol) was added excess *t*-Bu-4-pyridine (0.2 mL). The mixture was kept standing for several hours. After the remove of solvent and washing with hexanes, the yellow powder of **Pt2** was obtained in 90% yield (40 mg). ^{1}H NMR (400 MHz, C_6D_6, 25 °C, δ, ppm): 9.35 (s; 1H), 8.57 (dd, J = 5.2 Hz, J = 1.6 Hz; 2H), 8.18 (d, J = 8.0 Hz, 2H), 8.14 (d, J = 2.0 Hz; 1H), 7.67 (m; 2H), 7.60 (d, J = 8.0 Hz; 1H), 7.40 (m; 3H), 7.34 (d, J = 8.0 Hz; 1H), 7.12 (m; 1H), 7.05 (m; 2H), 6.94 (s; 4H), 6.65 (dd, J = 4.8 Hz, J = 1.6 Hz; 2H), 6.43 (t, J = 4.8 Hz; 1H), 2.27 (s; 12H), 2.21 (s; 6H), 0.87 (s; 9H). ^{13}C NMR was not recorded due to low solubility of the compound. Anal. Calcd for $C_{55}H_{54}BN_3Pt \cdot 0.5CH_2Cl_2$: C 66.30, H 5.51, N 4.18. Found: C 66.29, H 5.56, N 4.13.

Synthesis of ***Pt3***. Complex **Pt3** was synthesized using a modified procedure reported by M. E. Thompson and co-workers for the synthesis of Pt(ppy)(acac).[7a] A Pt(II) μ-dichloro-bridged dimer was synthesized first by heating the solution of K_2PtCl_4 with 2.2 equiv of **B1** in a 3:1 mixture of 2-ethoxyethanol and water at 80 °C for 30 h. This dimer was used directly in the next step without purification by reacting with 3 equiv of the chelating diketone (dpm) and 10 equiv of Na_2CO_3 in 2-ethoxyethanol at 100 °C for 30 h. Compound **Pt3** was isolated by column chromatography using CH_2Cl_2. A yellow solid of **Pt3** was recrystallized from CH_2Cl_2 and hexanes. The isolated yield for **Pt3** is 30%. ^{1}H NMR (400 MHz, CD_2Cl_2, 25 °C, δ, ppm): 9.02 (d, J = 4.8 Hz; 1H), 8.73 (d, J = 1.6; 1H), 8.26 (dd, J = 8.4 Hz, J = 2.0 Hz; 1H), 8.08 (d, J = 8.08; 1H), 7.86−7.92 (m; 2H), 7.82 (d, J = 2.0; 1H), 7.84 (dd, J = 5.6, J = 1.6; 1H), 7.69 (d, J = 7.6; 1H), 7.56 (d, J = 4.0 Hz; 1H); 7.29−7.32 (m; 2H), 7.17−7.23 (m; 2H), 6.62 (s; 4H), 5.85 (s; 1H), 2.14 (s; 6H), 1.82 (s; 12H), 1.29 (s; 9H), 1.21 (s, 9H). ^{13}C NMR (100 MHz, CD_2Cl_2, 25 °C, δ, ppm): 195.9, 194.3, 167.7, 157.9, 147.6, 146.1, 144.5, 141.7, 139.7, 138.8, 136.6, 136.5, 135.4, 134.1, 131.2, 131.1, 130.3, 129.3, 125.7, 124.0, 122.5, 122.4, 122.1, 119.3, 118.2, 111.3, 93.8, 41.9, 41.3, 35.0, 28.8, 28.5, 25.6, 25.4, 20.7. Anal. Calcd for $C_{51}H_{55}BN_2O_2Pt \cdot 0.5C_6H_{14}$: C 66.59, H 6.40, N 2.87. Found: C 66.48, H 6.74, N 2.80.

Molecular Orbital Calculations. DFT calculations were performed for **B1** and **Pt1**−**Pt3**. The geometrical parameters obtained for **B1** and **Pt3** from X-ray diffraction experiments were used as the starting point for their individual geometry optimization. The calculations were performed using the Gaussian03 package with the B3LYP/6-31G* basis set[10] for all atoms except Pt, for which LAN2LDZ was used. Time-dependent DFT (TD-DFT) calculations at the B3LYP level of theory were performed at the optimized ground-state geometry with the 6-31G* basis set for all atoms except Pt, for which LAN2LDZ was used. The TD-DFT calculation results can be found in the Supporting Information.

X-ray Crystallographic Analysis. Single crystals of **B1** and **Pt3** were obtained from a mixed solvent solution of CH_2Cl_2 and hexanes and mounted on glass fibers for data collection. Data were collected on a Bruker Apex II single-crystal X-ray diffractometer with graphite-monochromated Mo Kα radiation, operating at 50 kV and 30 mA and at 180 K. Data were processed on a PC with the aid of the Bruker SHELXTL software package (version 5.10)[11] and corrected for absorption effects. All non-hydrogen atoms were refined anisotropically. **Pt3** cocrystallizes with two CH_2Cl_2 solvent molecules in the crystal lattice, which were modeled and refined successfully. One of the *tert*-butyl groups in **Pt3** shows a rotational disordering with ~50% occupancy for each disordered site. This disordered group was modeled and refined successfully. Complete crystal structural data can be found in the Supporting Information. The crystal data of **B1** and **Pt3** have been deposited at the Cambridge Crystallographic Data Center (CCDC Nos. 830615, 830616).

RESULTS AND DISCUSSION

Syntheses and Structures. **B1** was synthesized by a Suzuki cross-coupling reaction between 2-(4-bromophenyl)pyridine and 4-(pyridin-2-yl)phenylboronic acid to produce **L1**. The use of 2-dicyclohexylphosphino-2′,6′-dimethoxybiphenyl in this cross-coupling reaction gave a better yield than other phosphines such as triphenylphosphine. Lithiation of **L1** followed by substitution with $BMes_2F$ provided **B1** (Scheme 1). The cyclometalated Pt(II) compound **Pt1** was obtained quantitatively by the reaction of **B1** and $PtPh_2(DMSO)_2$ in THF at 50 °C for 5 h through intramolecular C−H bond activation. Substitution of DMSO in **Pt1** with the stronger σ donor 4-*t*-Bu-pyridine quantitatively afforded **Pt2**. The Pt(dpm) cyclometalated compound **Pt3** was obtained in 30% yield using a modified procedure[7a] as reported by M. E. Thompson and co-workers for Pt(ppy)(acac), ppy = phenylpyridyl, by heating K_2PtCl_4 with 2.2 equiv of **B1** in a 3:1 mixture of 2-ethoxyethanol and water at 80 °C for 30 h, followed by the addition of 3 equiv of dipivaloylmethane (dpm) and 10 equiv of Na_2CO_3 in 2-ethoxyethanol at 100 °C for 30 h. **B1** and all Pt(II) complexes have been characterized by ^{1}H NMR and elemental analyses. The structures of **B1** and **Pt3** have been characterized by single-crystal X-ray diffraction analysis.

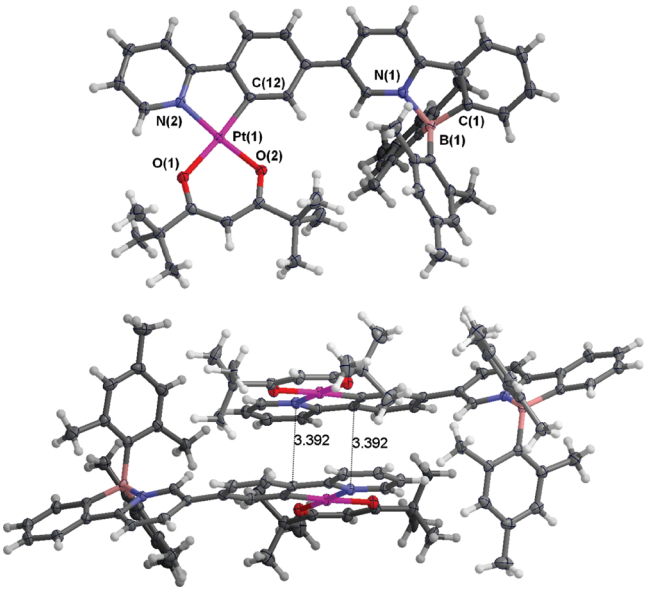

Figure 1. Diagrams showing the crystal structure of **Pt3** with 35% thermal ellipsoids (top) and the π-stacked dimer (bottom).

The crystal structure of **B1** can be found in the Supporting Information, and that of **Pt3** is shown in Figure 1. The geometry around the boron center in **Pt3** is similar to that of **B1** and those of our previously reported molecules such as **B1A**.[4] Compared to **B1**, the B−Mes bond distances in **Pt3** are notably longer (1.659(5) Å in **Pt3**, 1.645(2) Å in **B1**, on average). The B−N bond (1.654(4) Å) in **Pt3** is also notably longer than that of **B1** (1.6446(19) Å). This may be attributed to the greater steric congestion in the Pt(II) compound. Nonetheless, the B(ppy) unit and the Pt(ppy)(dpm) unit in **Pt3** adopt an approximately *syn* arrangement, with a dihedral angle of 40.9° between the two ppy units (the same dihedral angle is 36.0° for **B1**), as shown by the side view of the molecule in Figure 1 (bottom). The Pt(II) center has a typical square-planar geometry, with the Pt(1)−O(1) bond (2.068(2) Å) *trans* to the Pt(1)−C(12) bond being much longer than the Pt(1)−O(2) bond (2.006(2) Å) *trans* to the Pt−N bond, due to the greater *trans* influence exerted by the carbon donor. The Pt(1)···B(1) separation distance is 8.04(1) Å. Molecules of **Pt3** form a π-stacked dimer between the two Pt-ppy

dx.doi.org/10.1021/om200534m |*Organometallics* 2011, 30, 4453–4458

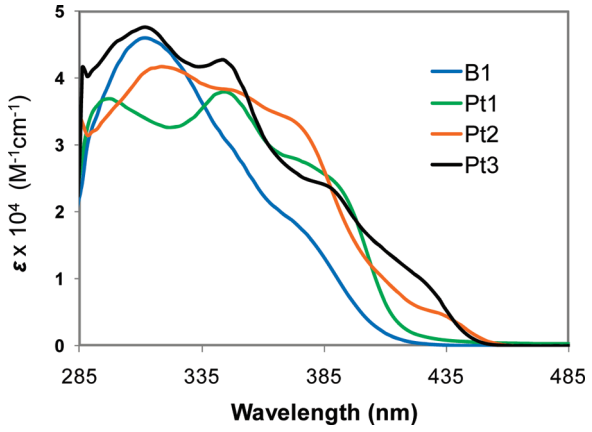

Figure 2. Absorption spectra of **B1** and complexes **Pt1**−**Pt3** in toluene at 298 K.

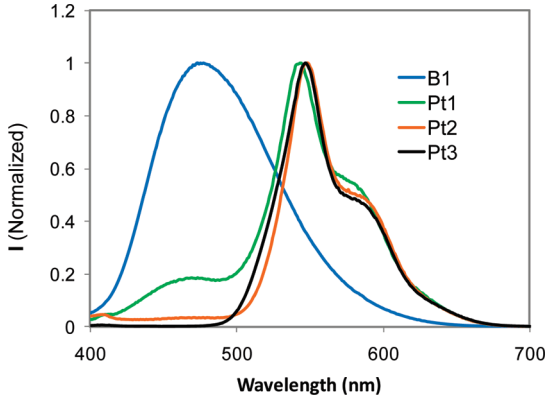

Figure 3. Fluorescence spectrum of **B1** and phosphorescence spectra of **Pt1**−**Pt3** in toluene (∼10^{-5} M) at 298 K under nitrogen.

chelate rings with the shortest separation distance being 3.392(4) Å. The Pt···Pt separation distance within the dimer is 5.181(2) Å. For **B1**, a π-stacked dimer was also observed in the crystal lattice, although the stacking is between the nonchelate ppy ring and the B-ppy chelate ring with much greater separation distances than those observed for **Pt3** (see Supporting Information).

Photophysical Properties. The absorption spectra of **B1** and the Pt(II) compounds are shown in Figure 2. **B1** has an intense band at ca. 320 nm, corresponding to π to π^* transition of the π-conjugated backbone, and a shoulder band at ca. 370 nm ascribed to the charge transfer (CT) transition from the mesityl groups to the π-conjugated backbone. On coordination to the Pt complexes system, this CT band shifts slightly to the red due to the Pt−C and Pt−N bond formation with the backbone, which extends the π conjugation of the backbone and lowers the LUMO level. Except the **Pt2** compound, which has a well-resolved low-energy MLCT band at ∼430 nm, the mesityl to the π-backbone CT band and the MLCT band are not resolved. On the basis of TD-DFT calculation results, the lowest energy band of **Pt1** at 410 nm is mainly CT from the mesityl to the backbone. The lowest energy transition of **Pt2** is a mixture of CT from the mesityl to the backbone and MLCT transitions, while for **Pt3** it is mostly CT from the mesityl to the backbone.

Compound **B1** displays blue-green fluorescence in toluene at ambient temperature with λ_{max} = 480 nm (Φ = 0.18) that

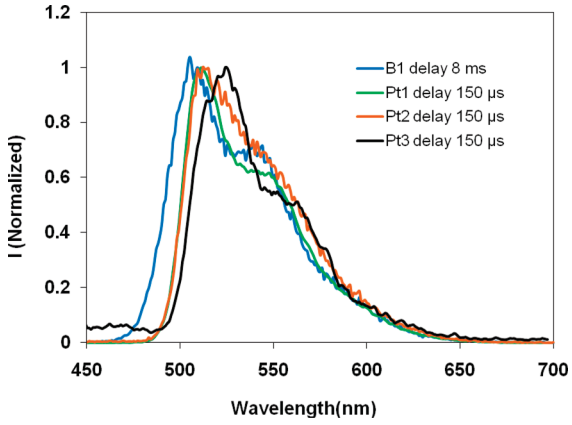

Figure 4. Time-resolved phosphorescence spectra of **B1** and Pt(II) compounds in toluene (∼10^{-5} M) at 77 K under nitrogen. The delay time used for each spectrum is indicated in the legend.

originates from the mesityl to the chelate backbone CT transition. All Pt(II) compounds exhibit bright and oxygen-sensitive phosphorescence (Figure 3). A phosphorescent emission band at 550 nm was observed for **Pt1** (Φ = 0.16, τ = 14.67(2) μs). In addition, **Pt1** has a high-energy shoulder band at 480 nm, which is attributed to the singlet emission of the chelate ligand due to its resemblance to the **B1** emission spectrum and its insensitivity toward oxygen (see Supporting Information). Only one intense emission band at 550 nm was observed for both **Pt2** (Φ = 0.13, τ = 9.64(5) μs) and **Pt3** (Φ = 0.45, τ = 14.5(1) μs). The well-resolved vibrational feature and the close resemblance of the emission spectra of the three Pt(II) compounds indicate that phosphorescence of these compounds is mostly ligand-centered emission (^{3}LC) with little involvement of MLCT transitions. This assignment is further supported by the time-resolved phosphorescence spectra recorded at 77 K (Figure 4). The phosphorescence of **B1** at 77 K has well-resolved vibrational features, thus may be attributed to a $\pi \rightarrow \pi^*$ transition localized on the conjugated backbone (^{3}LC), instead of the mesityl to backbone CT transition. The emission spectra of the metal compounds at 77 K have the same profile and are in a similar energy region to the phosphorescence spectrum of **B1** except a small red shift (∼5 nm for **Pt1** and **Pt2**, ∼20 nm for **Pt3**) due to cyclometalation, thus supporting that the low-energy emission band in all Pt(II) compounds is indeed ligand-centered phosphorescence (^{3}LC). Furthermore, the high phosphorescence efficiency of the Pt(II) compounds indicates that the backbone-based ^{3}LC emission is a highly effective deactivation pathway for the excited-state energy.

Photoisomerization. Upon excitation at 365 nm in toluene, the color of the **B1** solution becomes dark green with the appearance of a broad absorption band at 615 nm (Figure 5, Scheme 2), characteristic of photoisomerization around the boryl chromophore, forming the species **B1′**, as shown in Scheme 1. The formation of **B1′** via photolysis was also confirmed by NMR spectral data that have the characteristic chemical shifts of the dark isomer in related systems,[4] as we reported previously (see Supporting Information). The quantum yield for this photoisomerization process of **B1** at 298 K was determined to be ∼0.03 at 365 nm excitation, which is much lower than that of **B1A** ($\phi_{photoisomerization}$ = 0.85).[4b,c] Previously we have shown that the CT transition from a mesityl to the chelate backbone of B(ppy)Mes_2 (**B1A**) and its derivative is a key driving force for the isomerization process.[4] Extending the π-conjugation on the

dx.doi.org/10.1021/om200534m |*Organometallics* 2011, 30, 4453–4458

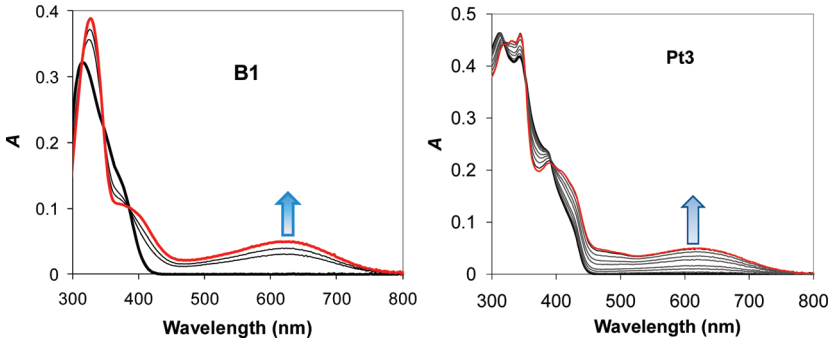

Figure 5. UV−vis spectral change of **B1** (left, total exposure time, 30 s) and **Pt3** (right, total exposure time, 35 min) in toluene (1.5×10^{-5} M) upon irradiation at 365 nm with a hand-held UV lamp.

Scheme 2.

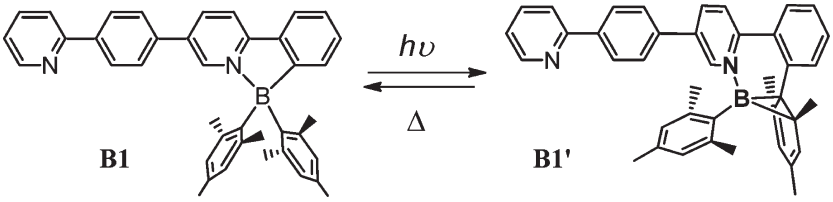

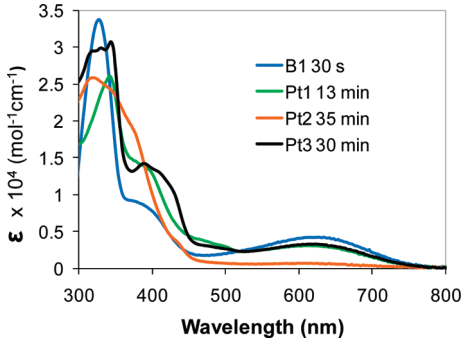

Figure 6. Comparison of the UV−vis spectral change of **B1** and complexes **Pt1**−**Pt3** in toluene (1.5×10^{-5} M) after irradiation at 365 nm for various time periods.

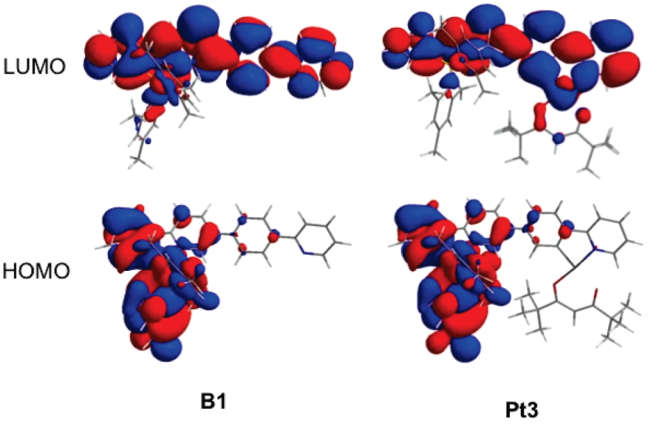

Figure 7. HOMO and LUMO (the major contributors in the lowest excited state) diagrams for **B1** and **Pt3** from DFT computational results. Details and diagrams for other compounds can be found in the Supporting Information.

backbone stabilizes the $\pi \rightarrow \pi^*$ transition state of the π-conjugated backbone such that it can become or approach the lowest excited state, thus competing with or partially quenching the CT state of the boryl chromophore and inhibiting the photoisomerization process. Indeed, TD-DFT computational results show that the lowest excited state of **B1** (HOMO to LUMO transition), albeit dominated by a mesityl to ppy charge transfer, has a significant contribution from the $\pi \rightarrow \pi^*$ transition of the π-conjugated backbone (Figure 7). We therefore believe that because of this the photoisomerization of **B1** is much less efficient than that of **B1A**. The photoisomerization of **B1** to **B1′** is fully thermally reversible.

All Pt(II) compounds undergo a similar photoisomerization process to that for **B1**, as confirmed by UV−vis and NMR spectra (see Supporting Information). Upon excitation of complexes **Pt1**, **Pt2**, and **Pt3** at 365 nm, a broad band that covers the 480 to 800 nm region arises as shown in Figures 5 and 6 (for complete photolysis data of each compound, please see Supporting Information), but at a much lower efficiency, compared to **B1**, despite the greater absorbance by the Pt(II) compounds at 365 nm. The quantum yields for photoisomerization of the Pt(II) compounds at 365 nm and 298 K were estimated to be ∼0.0015 for **Pt1**, <0.0001 for **Pt2**, and ∼0.0005 for **Pt3**. The low photoisomerization quantum efficiencies of the Pt(II) compounds can be attributed to the low-lying ^{3}LC state that becomes an effective deactivation pathway due to the efficient spin−orbit coupling and the singlet−triplet intersystem crossing imposed by Pt(II) chelation, as supported by the highly efficient ^{3}LC phosphorescence of these compounds. This finding also supports that photoisomerization of the B(ppy)Mes$_2$ chromophore is most likely through the singlet CT state. Furthermore, on the basis of the absorption spectral data and TD-DFT computational

dx.doi.org/10.1021/om200534m |*Organometallics* 2011, 30, 4453–4458

results, it appears that the greater the involvement of MLCT in the lowest electronic transition, the less efficient the photoisomerization since **Pt2** is the least efficient in photoisomerization but with the most significant contributions of MLCT to the lowest excited state, compared to **Pt1** and **Pt3** (see Supporting Information). Hence a low-lying MLCT state is also a highly effective deactivation pathway for photoisomerization of the boryl chromophore in the metal compounds.

The behavior of the B(ppy)Mes_2 system is in sharp contrast to that of dithienylethene compounds, which have been shown to undergo photoisomerization from a LC excited state that may be sensitized by the attachment of a metal ion via an energetically favorable MLCT excited state, as demonstrated by a number of research groups.[6]

■ CONCLUSIONS

A new photochromic boryl compound that is capable of forming cyclometaled Pt(II) compounds has been achieved. Three cyclometalated Pt(II) compounds that share a conjugated chelate backbone with the photochromic chromophore B(ppy)Mes_2 have been synthesized. These Pt(II) compounds are brightly phosphorescent at ambient temperature. The Pt(II) unit in these compounds has been found to be highly effective in quenching the photoisomerization process of the B(ppy)Mes_2 chromophore by enhancing the ^{3}LC state localized on the chelate backbone. On the basis of this study, enhancing the mesityl to the chelate charge transfer transition and destabilizing the $\pi \rightarrow \pi^*$ transition of the chelate backbone are the key factors that should be considered for achieving new and highly efficient photochromic systems based on N,C-chelate four-coordinate boron compounds.

■ ASSOCIATED CONTENT

Supporting Information. Synthetic details for the precursor compounds of **L1**, phosphorescence spectral change of Pt(II) compounds toward oxygen, TD-DFT computational data and MO diagrams, photoisomerization experimental details and data, and complete crystal structural data. This material is available free of charge via the Internet at http://pubs.acs.org.

■ AUTHOR INFORMATION

Corresponding Author

*E-mail: wangs@chem.queensu.ca.

■ ACKNOWLEDGMENT

We thank the Natural Sciences and Engineering Research Council of Canada for financial support.

■ REFERENCES

(1) For recent reviews, see: (a) Rao, Y. L; Wang, S. *Inorg. Chem.* **2011**ASAP and references therein. (b) Wang, S. *Coord. Chem. Rev.* **2001**, *215*, 79. (c) Entwistle, C. D.; Marder, T. B. *Angew. Chem., Int. Ed.* **2002**, *41*, 2927. (d) Entwistle, C. D.; Marder, T. B. *Chem. Mater.* **2004**, *16*, 4574. (e) Fukazawa, A.; Yamaguchi, S. *Chem. Asian J.* **2009**, *4*, 1386. (f) Loudet, A.; Burgess, K. *Chem. Rev.* **2007**, *107*, 4891. (g) Jäkle, F. *Chem. Rev.* **2010**, *110*, 3985. (h) Jäkle, F. *Coord. Chem. Rev.* **2006**, *250*, 1107.

(2) (a) Cui, Y.; Liu, Q. D.; Bai, D. R.; Jia, W. L.; Tao, Y.; Wang, S. *Inorg. Chem.* **2005**, *44*, 601. (b) Liu, S. F.; Wu, Q.; Schmider, H. L.; Aziz, H.; Hu, N.-X.; Popović, Z.; Wang, S. *J. Am. Chem. Soc.* **2000**, *122*, 3671. (c) Liu, Q.-D.; Mudadu, M. S.; Thummel, R.; Tao, Y.; Wang, S. *Adv. Funct. Mater.* **2005**, *15*, 143. (d) Chen, H.-Y.; Chi, Y.; Liu, C.-S.; Yu, J.-K.; Cheng, Y.-M.; Chen, K.-S.; Chou, P.-T.; Peng, S.-M.; Lee, G.-H.; Carty, A. J.; Yeh, S.-J.; Chen, C.-T. *Adv. Funct. Mater.* **2005**, *15*, 567. (e) Zhang, H.; Huo, C.; Zhang, J.; Zhang, P.; Tian, W.; Wang, Y. *Chem. Commun.* **2006**, 281. (f) Zhang, Z.; Bi, H.; Zhang, Y.; Yao, D.; Gao, H.; Fan, Y.; Zhang, H.; Wang, Y.; Wang, Y.; Chen, Z.; Ma, D. *Inorg. Chem.* **2009**, *48*, 7230.

(3) (a) Zhang, G.; Lu, J.; Sabat, M.; Fraser, C. L. *J. Am. Chem. Soc.* **2010**, *132*, 2160. (b) Zhang, G.; Palmer, G. M.; Dewhirst, M. W.; Fraser, C. L. *Nat. Mater.* **2009**, *8*, 747. (c) Maeda, H.; Mihashi, Y.; Haketa, Y. *Org. Lett.* **2008**, *10*, 3179. (d) Maeda, H.; Haketa, Y. *Pure Appl. Chem.* **2011**, *83*, 189. (e) Kano, N.; Yoshino, J.; Kawashima, T. *Org. Lett.* **2005**, *7*, 3909. (f) Yoshino, J.; Kano, N.; Kawashima, T. *Tetrahedron* **2008**, *64*, 7774.

(4) (a) Rao, Y. L.; Amarne, H.; Zhao, S. B.; McCormick, T. M.; Martić, S.; Sun, Y.; Wang, R. Y.; Wang, S. *J. Am. Chem. Soc.* **2008**, *130*, 12898. (b) Baik, C.; Hudson, Z. M.; Amarne, H.; Wang, S. *J. Am. Chem. Soc.* **2009**, *131*, 14549. (c) Amarne, H.; Baik, C.; Murphy, S. K.; Wang, S. *Chem.—Eur. J.* **2010**, *16*, 4750. (d) Murphy, S. K.; Baik, C.; Lu, J. S.; Wang, S. *Org. Lett.* **2010**, *12*, 5266. (e) Amarne, H.; Baik, C.; Wang, R.; Wang, S. *Organometallics* **2011**, *30*, 665. (f) Baik, C.; Murphy, S. K.; Wang, S. *Angew. Chem., Int. Ed.* **2010**, *49*, 8224.

(5) Kume, S.; Nishihara, H. *Dalton Trans.* **2008**, 3260 and references therein.

(6) (a) Yam, V. W.-W.; Ko, C.-C.; Zhu, N. *J. Am. Chem. Soc.* **2004**, *126*, 12734. (b) Yam, V. W.-W.; Ko, C.-C.; Zhu, N. *J. Am. Chem. Soc.* **2007**, *129*, 6058. (c) Ko, C.-C.; Wu, L.-X.; Wong, M.-C. K.; Zhu, N.; Yam, V. W.-W. *Chem.—Eur. J.* **2004**, *10*, 766. (d) Yam, V. W.-W.; Ko, C.-C.; Wu, L.-X.; Wong, M.-C. K.; Cheung, K.-K. *Organometallics* **2000**, *19*, 1820. (e) Ko, C.-C.; Yam, V. W.-W. *J. Mater. Chem.* **2010**, *20*, 2063. (f) Roberts, M. N.; Carling, C.-J.; Nagle, J. K.; Branda, N. R.; Wolf, M. O. *J. Am. Chem. Soc.* **2009**, *131*, 16644. (g) Aubert, V.; Guerchais, V.; Ishow, E.; Hoang-Thi, K.; Ledoux, I.; Nakatani, K.; Le Bozec, H. *Angew. Chem., Int. Ed.* **2008**, *47*, 577. (h) Belser, P.; De Cola, L.; Hartl, F.; Adamo, V.; Bozic, B.; Chriqui, Y.; Iyer, V. M.; Jukes, R. T. F.; Kühni, J.; Querol, M.; Roma, S.; Salluce, N. *Adv. Funct. Mater.* **2006**, *16*, 195.

(7) (a) Brooks, J.; Babayan, Y.; Lamansky, S.; Djurovich, P. I.; Tsyba, I.; Bau, R.; Thompson, M. E. *Inorg. Chem.* **2002**, *41*, 3055. (b) Hudson, M. Z.; Sun, C.; Helander, M. G.; Amarne, H.; Lu, Z.-H.; Wang, S. *Adv. Funct. Mater.* **2010**, *20*, 3426. (c) Rao, Y. L.; Wang, S. *Inorg. Chem.* **2009**, *48*, 7698.

(8) Klein, A.; Schurr, T.; Knödler, A.; Gudat, D.; Klinkhammer, K.-W.; Jain, V. K.; Zalis, S.; Kaim, W. *Organometallics* **2005**, *17*, 4125.

(9) Sajoto, T.; Djurovich, P. I.; Tamayo, A. B.; Oxgaard, J.; Goddard, W. A., III; Thompson, M. E. *J. Am. Chem. Soc.* **2009**, *131*, 9813.

(10) Frisch, M. J.; et al. *Gaussian 03*, Revision C.02; Gaussian, Inc.: Wallingford, CT, 2004.

(11) *SHELXTL* Version 6.14; Bruker AXS, 2000−2003.